Earthline Journal of Mathematical Sciences
E-ISSN: 2581-8147
Volume 15, Number 5, 2025, Pages 849-872
https://doi.org/10.34198/ejms.15525.849872

Sensitivity Analysis of a Mathematical Model for Tuberculosis-Schistosomiasis Model with Vaccination and Treatment

I. I. Ako[1,*] and R. U. Omoregie[2]

[1] Department of Mathematics, University of Benin, Benin City, Nigeria
e-mail: ignatius.ako@uniben.edu

[2] Department of Mathematics, University of Benin, Benin City, Nigeria
e-mail: rosemary.akhaze@uniben.edu

Abstract

Herein, we investigate the uncertainty and sensitivity analysis of the effective reproduction number belonging to a tuberculosis-schistosomiasis co-infection model which harbours both vaccination and treatment as espoused by Ako and Omoregie [3]. The results gleaned from some of the contour plots showed that the impact of the treatment levels for individuals with infectious TB on the burden of tuberculosis in a population, is largely determined by the efficacy of the BCG vaccine on vaccinated individuals. Furthermore, just as obtained in Ako [1], the impact of the fraction of individuals who progress to infectious TB via the fast route is also determined by the proportion of individuals unvaccinated with the BCG vaccine. Furthermore, contour plots suggest that the effect of the cercarial production, cercarial penetration, the number of schistosome eggs secreted and the successful conversion of the eggs to miracidia, on the hardship of tuberculosis in a populace, is predominantly determined by the medical care levels for individuals with active schistosomiasis. Hence, public health policy should take into account the level of medical care facilities available. With increasing (and sustained) treatment rates for schistosomiasis infections, having a large proportion of active schistosomiasis patients expeditiously receiving medical care will result in a reduction in the disease hardship in the populace.

1 Introduction

Tuberculosis (TB), engendered by bacteria known as *Mycobacterium tuberculosis* mostly affects the pulmonary apparatus, is an airborne disease spread when people with pulmonary TB spit, sneeze or cough. It is estimated that 10 million persons take ill with TB yearly [44, 46]. Even though TB is both preventable and curable, about 1.5 million people suffer mortality as a result of contracting the disease

Received: June 1, 2025; Accepted: July 8, 2025; Published: July 30, 2025
2020 Mathematics Subject Classification: 93B99.
Keywords and phrases: tuberculosis, schistosomiasis, reproduction number, uncertainty, sensitivity analysis.
*Corresponding author

granting it a status of the world's number one infectious killer [46]. Specifically, in 2023, 1.25 million persons died from TB inclusive of 161,000 individuals living with HIV; it was also estimated that 10.8 million took ill with TB globally that same year [44, 46]. TB, obviously, is the leading cause of death of individuals with HIV/AIDS and is a major purveyor of antimicrobial resistance [46]. TB is found globally with half of cases found in eight nations: China, Bangladesh, India, Pakistan, Indonesia, Nigeria, Philippines and South Africa [46]. People infected with the disease have a 5% - 10% lifetime risk of getting sick with TB [46]. The common symptoms of TB are: chest pain, prolonged cough, weakness or fatigue, weight loss, fever and night sweats [46].

Schistosomiasis is described as an acute and chronic parasite disease propagated by blood flukes of the genus *Schistosoma* and with human infections precipitated by several identified activities that provide the opportunity for contact with infested water bodies [45]. It was estimated, in 2021, that about 251 million plus persons needed preventive therapy [45, 46]. About 78 nations have reported cases of schistosomiasis so far [46]. Co-infection/co-endemicity of TB and schistosomiasis have been established in the literature [1, 2, 23].

Many authors have enriched the literature via mathematical modeling of TB [6, 7, 9, 16, 28, 30–34, 43] and schistosomiasis [10, 12, 13, 15, 17, 18, 21, 22, 24, 27, 35–37, 39, 40, 49], respectively. However, Ako and Olowu pioneered the mathematical modeling and analysis of TB-schistosomiasis co-infectionm [2]. Ako and Omoregie [3] further introduced and investigated the impact of vaccination and treatment to the work of [2]. Currently, in this study, we seek to carry out uncertainty and sensitivity analysis of some significant parameters *viz-á-vis* the effective reproductive ratio computed for the work of Ako and Omoregie [3] [8,11].

This article is organized as follows: we review the model formulation in [3] in Section 2. Section 3 has to do with both the qualitative and quantitative mathematical analysis of the effective reproduction number. Uncertainty and sensitivity analysis of some significant parameters of the effective reproduction number are treated in Section 4. Section 5 gives the conclusion.

2 Model Formulation [3]

At this juncture, we consider the tuberculosis-schistosomiasis co-infection model with imperfect TB (BCG) vaccine and treatment developed by [3]. The complete human population at time t, given by $N_H(t)$, is split into sixteen mutually exclusive categories comprising of individuals susceptible to infections ($S_H(t)$), vaccinated with BCG ($V_T(t)$) , humans vaccinated with BCG and exposed to schistosomiasis ($V_{TS}(t)$), with latent TB but not infectious ($E_{HT}(t)$), infectious TB ($I_{HT}(t)$), exogenously re-infected with TB ($I_{RT}(t)$), treated for TB ($T_{HT}(t)$), exposed to schistosomiasis ($E_{HS}(t)$), infected with schistosomiasis ($I_{HS}(t)$), treated for schistosomiasis ($T_{HS}(t)$), exposed to TB, exposed to schistosomiasis ($E_{TS}(t)$), with active

TB, exposed to schistosomiasis ($I_{ST}(t)$), exogenously re-infected with TB, exposed to schistosomiasis ($I_{RS1}(t)$), exposed to TB, with active schistosomiasis ($E_{ST}(t)$), exogenously re-infected with TB and active schistosomiasis (I_{RS2}), and with infectious TB, active schistosomiasis ($I_{TS}(t)$) humans remain the same, such that the total human population is represented by

$$\begin{aligned} N_H(t) = {} & S_H(t) + V_T(t) + V_{TS}(t) + E_{HT}(t) + I_{HT}(t) + I_{RT}(t) + T_{HT}(t) \\ & + E_{HS}(t) + I_{HS}(t) + T_{HS}(t) + E_{TS}(t) + I_{ST}(t) + I_{RS1}(t) \\ & + E_{ST}(t) + I_{RS2}(t) + I_{TS}(t). \end{aligned} \tag{2.1}$$

Incorporating the pathogen responsible for schistosomiasis into the co-infection dynamics, we assume that the miracidia and cercariae population at the different stages in the life-cycle of the *Schistosoma spp* are depicted by $L(t)$ and $J(t)$ compartments respectively. Next, we incorporate the intermediary hosts, freshwater snails, for the pathogen responsible for schistosomiasis in the model formulation. We presume that the entire snail populace in the freshwater environment at time t, given by $N_S(t)$, is broken down into the jointly exclusive classes of susceptible snails ($S_S(t)$) and snails penetrated with miracidia ($I_S(t)$), where

$$N_S(t) = S_S(t) + I_S(t). \tag{2.2}$$

The parameters unique to vaccination model are assembled in Table 2, whereas the numerical sizes and ranges of the parameters used for the simulation on the model (2.3) are showcased in Tables 4 and 5, respectively.

$$
\begin{aligned}
S'_H &= \omega\Lambda_H + \theta_V V_T - \lambda_T S_H - \lambda_J S_H - \mu_H S_H,\\
V'_T &= (1-\omega)\Lambda_H - \lambda_J V_T - (1-\epsilon_1)\lambda_T V_T - (\theta_V + \mu_H)V_T,\\
V'_{TS} &= \lambda_J V_T - \zeta_{TS}\lambda_T V_{TS} - \mu_H V_{TS},\\
E'_{HT} &= (1-p)\lambda_T(S_H + \xi T_{HT} + T_{HS}) + (1-\epsilon_1)\lambda_T V_T + \zeta_{S1}E_{ST}\\
&\quad - (1-\pi_1)\lambda_T E_{HT} - \lambda_J E_{HT} - (\kappa_1 + \mu_H)E_{HT},\\
I'_{HT} &= p\lambda_T(S_H + \xi T_{HT} + T_{HS}) + \kappa_1 E_{HT} + \zeta_{S3}I_{TS} - \lambda_J I_{HT}\\
&\quad - (\zeta_T + \delta_T + \mu_H)I_{HT},\\
I'_{RT} &= (1-\pi_1)\lambda_T E_{HT} + \zeta_{S2}I_{RS2} - \lambda_J I_{RT} - (\zeta_R + \delta_R + \mu_H)I_{RT},\\
T'_{HT} &= \zeta_T I_{HT} + \zeta_R I_{RT} - \xi\lambda_T T_{HT} - \lambda_J T_{HT} - \mu_H T_{HT},\\
E'_{HS} &= \lambda_J(S_H + T_{HT} + \psi T_{HS}) + \zeta_{T1}I_{ST} + \zeta_{R1}I_{RS1} - \eta_1\lambda_T E_{HS}\\
&\quad - (\alpha_1 + \mu_H)E_{HS},\\
I'_{HS} &= \alpha_1 E_{HS} + \zeta_{T2}I_{RS2} + \zeta_{T3}I_{TS} - \eta_2\lambda_T I_{HS} - (\zeta_S + \delta_S + \mu_H)I_{HS},\\
T'_{HS} &= \zeta_S I_{HS} - \lambda_T T_{HS} - \psi\lambda_J T_{HS} - \mu_H T_{HS},\\
E'_{TS} &= (1-m)\eta_1\lambda_T E_{HS} + \lambda_J E_{HT} + \zeta_{TS}V_{TS}\lambda_T - (1-\pi_2)\lambda_T E_{TS}\\
&\quad - (\alpha_2 + \kappa_2 + \mu_H)E_{TS},\\
I'_{ST} &= m\eta_1\lambda_T E_{HS} + \lambda_J I_{HT} + \lambda_J I_{RT} + \kappa_2 E_{TS} - (\zeta_{T1} + \sigma + \chi_1\delta_T + \mu_H)I_{ST},\\
I'_{RS1} &= (1-\pi_2)\lambda_T E_{TS} - (\alpha_3 + \zeta_{R1} + \tau_1\delta_R + \mu_H)I_{RS1},\\
E'_{ST} &= (1-f)\eta_2\lambda_T I_{HS} + \alpha_2 E_{TS} - (1-\pi_3)\lambda_T E_{ST} - (\zeta_{S1} + \kappa_3 + v_1\delta_S + \mu_H)E_{ST},\\
I'_{RS2} &= (1-\pi_3)\lambda_T E_{ST} + \alpha_3 I_{RS1} - (\zeta_{T2} + \zeta_{S2} + \tau_2\delta_R + v_2\delta_S + \mu_H)I_{RS2},\\
I'_{TS} &= f\eta_2\lambda_T I_{HS} + \kappa_3 E_{ST} + \sigma I_{ST} - (\zeta_{T3} + \zeta_{S3} + \chi_2\delta_T + v_3\delta_S + \mu_H)I_{TS},\\
L' &= N_e\gamma(I_{HS} + E_{ST} + I_{RS2} + I_{TS}) - \mu_L L,\\
S'_S &= \Lambda_S - \lambda_L S_S - \mu_S S_S,\\
I'_S &= \lambda_L S_S - \mu_S I_S,\\
J' &= \phi I_S - \mu_J J.
\end{aligned}
\tag{2.3}
$$

where

$$
\begin{aligned}
\lambda_T &= \frac{\beta_T(I_{HT} + \Theta_{RT}I_{RT} + \Theta_{RS1}I_{RS1} + \Theta_{RS2}I_{RS2} + \Pi_1 I_{ST} + \Pi_2 I_{TS})}{N_H},\\
\lambda_J &= \frac{\beta_J J}{J_0 + \epsilon J}, \qquad \lambda_L = \frac{\beta_L L}{L_0 + \epsilon L}.
\end{aligned}
\tag{2.4}
$$

Table 1: Description of state variables of the model (2.3) [3].

State Variables	Description
$S_H(t)$	Susceptible human population
V_T	Human population vaccinated with BCG
V_{TS}	Human population vaccinated with BCG and exposed to schistosomiasis
$E_{HT}(t)$	Human population with dormant TB
$I_{HT}(t)$	Human population with virulent TB
$I_{RT}(t)$	Human population exogenously infected with TB
$T_{HT}(t)$	Human population treated for TB
$E_{HS}(t)$	Human population unprotected against schistosomiasis
$I_{HS}(t)$	Human population contaminated with schistosomiasis
$T_{HS}(t)$	Human population cured of schistosomiasis
$E_{TS}(t)$	Human population unprotected against both TB and schistosomiasis
$I_{ST}(t)$	Human population with active TB and unprotected against schistosomiasis
$I_{RS1}(t)$	Human population externally infected with TB and unprotected against schistosomiasis
$E_{ST}(t)$	Human population unprotected against TB and virulent schistosomiasis
$I_{RS2}(t)$	Human population externally infected with TB and active schistosomiasis
$I_{TS}(t)$	Human population with contagious TB and active schistosomiasis
$L(t)$	Miracidia (parasite larvae immediately after hatching from the eggs) population
$S_S(t)$	Susceptible snail populace
$I_S(t)$	Snail populace contaminated with miracidia in the marine environment
$J(t)$	Cercariae (larvae in the water that pierces the human skin) populace

3 Local Asymptotic Stability of Disease-Free Equilibrium (DFE) [3]

The model system (2.3) in [3] has a DFE given by

$$\begin{aligned}\mathcal{E}_o &= (S_H^*, V_T^*, V_{TS}^*, E_{HT}^*, I_{HT}^*, I_{RT}^*, T_{HT}^*, E_{HS}^*, I_{HS}^*, T_{HS}^*, E_{TS}^*, I_{ST}^*, I_{RS1}^*, E_{ST}^*, \\ &\quad I_{RS2}^*, I_{TS}^*, L^*, S_S^*, I_S^*, J^*) \\ &= (\frac{(\theta_V + \omega\mu_H)\Lambda_H}{(\theta_V + \mu_H)\mu_H}, \frac{(1-\omega)\Lambda_H}{(\theta_V + \mu_H)}, 0, 0, 0, 0, 0, 0, 0, 0, 0, 0, 0, 0, 0, 0, 0, \frac{\Lambda_S}{\mu_S}, 0, 0).\end{aligned}$$

Table 2: Description of state variables of the model (2.3) [3]

Parameters	Description
Λ_H	Human recruitment rate
μ_H	Human natural mortality rate
β_T	TB transmission rate
ξ	Reduced rate of infection with TB, $\xi \leq 1$
f, m, p	Proportion of fast progressors to TB
π_1, π_2, π_3	Exogenous re-infection rates, where $0 \leq \pi_1, \pi_2, \pi_3 \leq 1$
$\kappa_1, \kappa_2, \kappa_3$	Endogenous reactivation rates
$\zeta_T, \zeta_{T1}, \zeta_{T2}, \zeta_{T3}, \zeta_R, \zeta_{R1}$	Therapeutic rates for TB
δ_T, δ_R	TB-influenced human death rates
ψ	Lowered rate of contagion with schistosomiasis
α_1	Advancement rate from dormant to virulently tainted with schistosomiasis
α_2	Advancement rate from unprotected against both TB/schistosomiasis to unprotected against TB/virulent schistosomiasis
α_3	Advancement rate from externally re-tainted with TB-/unprotected against schistosomiasis to externally re-tainted with TB-/virulent schistosomiasis
$\zeta_S, \zeta_{S1}, \zeta_{S2}, \zeta_{S3}$	Therapeutic rates for schistosomiasis
δ_S	Schistosomiasis-influenced human mortality rate
σ	Advancement rate from virulent TB/unprotected against schistosomiasis to virulent TB/virulent schistosomiasis
χ_1, χ_2	Modification parameters for elevated TB mortality as a consequence of co-infection
η_1, η_2	Adjustment parameters for the rate at which humans with dormant and virulent schistosomiasis are infected with TB
$\Theta_{RT}, \Theta_{RS1}, \Theta_{RS2}$	Adjustment parameters for comparative infectiousness of re-infected humans
Π_1, Π_2	Adjustment parameters for comparative contagiousness of humans with virulent TB and dormant/virulent schistosomiasis
τ_1, τ_2	Modification parameters for elevated TB deaths to external re-tainting as a result of co-infection
v_1, v_2, v_3	Adjustment parameters for schistosomiasis-induced deaths
Λ_S	Enrollment rate for snail population
μ_S	Snail mortality rate
ϵ	Growth velocity limitation
L_0	Saturation constant for the miracidia
β_L	Miracidial contagion rate
N_e	Statistic of eggs excreted by people

Table 3: Description of state variables of the model (2.3) [3].

Parameters	Description
ω	Proportion unvaccinated with BCG against TB
$1-\epsilon_1$	Reduction in BCG vaccine efficacy
θ_V	Vaccine waning
ζ_{TS}	Impact of schistosomiasis on the BCG protection against TB, $\zeta_{TS} \geq 1$

It can be shown, employing the next-generation operator method (van den Driessche and Watmough, 2002), that the associated effective reproduction number of the model (2.3), $\mathcal{R}_{TS}^V$, is given by

$$\mathcal{R}_{TS}^V = max\left\{\mathcal{R}_{HT}^V, \mathcal{R}_{HS}\right\}, \tag{3.1}$$

where

$$\mathcal{R}_{HT}^V = \frac{\beta_T\left(\theta_V(\kappa_1 + p\mu_H) + \mu_H((1-(1-\omega)\epsilon_1)\kappa_1 + p\omega\mu_H)\right)}{(\kappa_1+\mu_H)(\zeta_T+\delta_T+\mu_H)(\theta_V+\mu_H)},$$

$$\mathcal{R}_{HS} = \sqrt{\frac{\alpha_1\beta_J\beta_L\Lambda_H\Lambda_S N_e\gamma\phi}{J_0L_0\mu_H\mu_J\mu_L\mu_S^2(\alpha_1+\mu_H)(\zeta_S+\delta_S+\mu_H)}}$$

are the *effective reproduction number* for TB and schistosomiasis, respectively.

Utilising Theorem 2 in van den Driessche and Watmough (2002), we establish the following conclusion:

Lemma 3.1. *The DFE $\mathcal{E}_0$ is locally asymptotically stable (LAS) in $\mathcal{D}$ if $\mathcal{R}_{TS}^V < 1$ and unstable if $\mathcal{R}_{TS}^V > 1$.*

The threshold quantity, $\mathcal{R}_{TS}^V$, is a measure of the average number of secondary infections engendered by a single infected person in a wholly susceptible population, where a fraction of the susceptible human population is vaccinated using an imperfect TB (BCG) vaccine.

3.1 Analysis of $\mathcal{R}_{TS}^V$

Analysis of the threshold quantity, $\mathcal{R}_{TS}^V$, with respect to some key parameters ($\omega, \zeta_T, \zeta_S, N_e, \gamma, \phi, J_0$ and L_0) is investigated by considering the partial derivatives of $\mathcal{R}_{TS}^V$ corresponding to these parameters.

3.1.1 Analysis of $\mathcal{R}_{HT}^{V}$

Calculating the partial derivatives of $\mathcal{R}_{HT}^{V}$ with respect to some of the parameters under scrutiny (ω and ζ_T) exposes the consequence of these parameters on TB regulation in the populace. This gives

$$\frac{\partial \mathcal{R}_{HT}^{V}}{\partial \omega} = \frac{\beta_T \epsilon_1 \kappa_1 \mu_H}{(\theta_V + \mu_H)(\kappa_1 + \mu_H)(\zeta_T + \delta_T + \mu_H)} > 0. \tag{3.2}$$

Apparently, it ensues from (3.2) that the partial derivative is greater than zero, unconditionally. Hence, the proportion of unvaccinated susceptible individuals will have a negative impact in decreasing the burden of TB in the community, regardless of the values of the other parameters in the expression on the right-hand side of (3.2) .

$$\frac{\partial \mathcal{R}_{HT}^{V}}{\partial \zeta_T} = -\frac{\mathcal{R}_{HT}^{V}}{(\zeta_T + \delta_T + \mu_H)} < 0. \tag{3.3}$$

Certainly, it follows from (3.3) that the partial derivative is negative, unconditionally. Thus, effective treatment rate of TB at the phase of infection will exert a positive impact in decreasing the burden of TB in the community, irrespective of the values of the other parameters in the expression on the right-hand side of (3.3).

Further analysis of $\mathcal{R}_{HT}^{V}$ yields

$$\lim_{\substack{\omega \to 0 \\ \zeta_T \to \infty}} \mathcal{R}_{HT}^{V} = 0 \tag{3.4}$$

The limit in (3.4) demonstrates the impact of a TB regulation plan that concentrates on adequate vaccination of a very sizeable proportion of the susceptible individuals with BCG with very high efficacy, prompt treatment of humans with active TB.

From the analysis of $\mathcal{R}_{HT}^{V}$ as seen in (3.2) - (3.3) and (3.4), respectively, we obtain the following results:

Lemma 3.2. *The effective treatment rate (ζ_T) for the infectious stage of infection, as a result of fast progression, will exert a positive impact in decreasing the TB burden in a populace, regardless of the values of the other parameters in the effective reproduction number; whereas, the proportion of unvaccinated susceptible individuals with BCG vaccination rate (ω) will exert a negative impact in reducing the TB burden in a populace. Hence, any intervention strategy which concentrates on vaccination a larger fraction*

of the susceptible population and prompt and effective treatment of infectious TB cases will exert a positive effect on decreasing the overall TB burden in the populace.

Further analysis of the threshold quantity, $\mathcal{R}_{HT}^{V}$, is carried out by investigating its sensitivity to certain key parameters, namely: the treatment rate (ζ_T), the proportion of unvaccinated individuals (ω), the BCG vaccine efficacy (ϵ_1), as well as the fraction or proportion of fast progressors to TB (p). Hence , we examine the contour plots (Figures 1 - 2) of $\mathcal{R}_{HT}^{V}$ as functions of ζ_T, β_T, κ_1 and p. The values of the parameters used for generating the contour plots are obtained from Tables 4 and 5.

The plot in Figure 1 indicates that a very high treatment level ($\zeta_T = 0.75$) and high efficacy of the BCG vaccine ($\epsilon_1 = 0.9$) given that the disease transmission rate is $\beta_T = 1.5$, is required to eradicate TB from the population. Effective treatment of about 85% of actively-infected individuals and BCG vaccine efficacy of about 80% is required to annihilate TB from the population. Any regulatory policy hinged on the measures presented in Figure 1 will compel $\mathcal{R}_{HT}^{V}$ to acquire a value below unity.

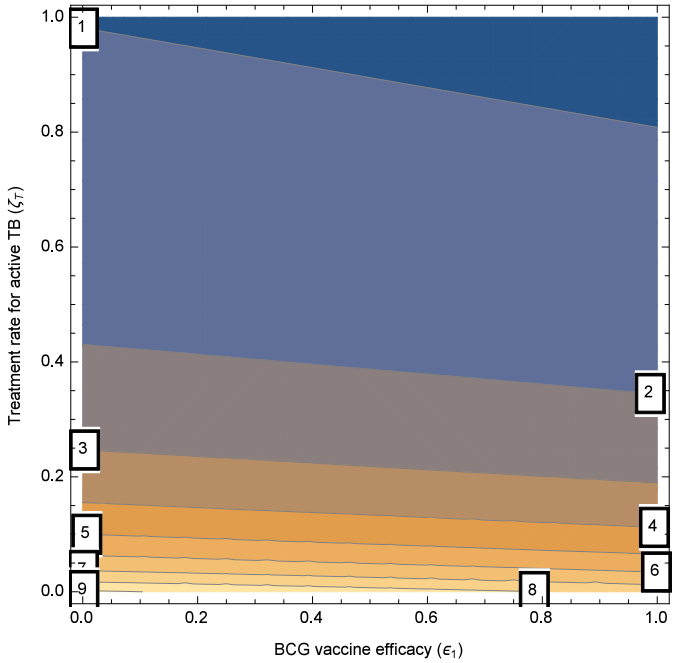

Figure 1: Contour plot of $\mathcal{R}_{HT}^{V}$ as a function of ζ_T and ϵ_1, when $\zeta_T = 0.75$ and $\epsilon_1 = 0.9$ and $\beta_T = 1.5$.

Figure 2 suggests that it will be extremely difficult to abolish TB from the populace due to the presence of unvaccinated individuals in the human population ($\omega = 0.2$) and the fraction of individuals who progress to infectious TB via the fast route ($p = 0.1$), regardless of intervention via treatment for cases with active TB and the vaccination of susceptible individuals with the BCG vaccine.

In summary, the results from these contour plots above suggest that the impact of the treatment levels

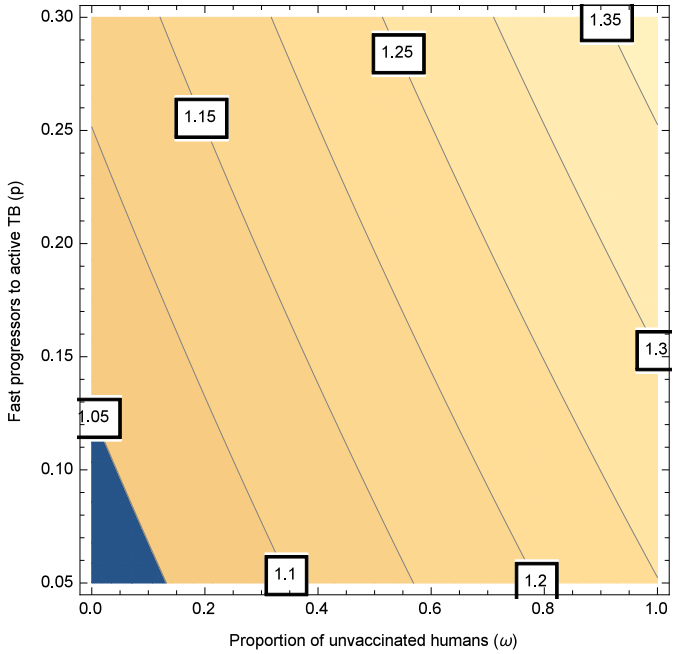

Figure 2: Contour plot of $\mathcal{R}_{HT}^{V}$ as a function of ω and p, when $\omega = 0.2$ and $p = 0.1$ and $\beta_T = 1.5$.

for individuals with infectious TB on the burden of tuberculosis in a population, is largely determined by the efficacy of the BCG vaccine on vaccinated individuals. Furthermore, the impact of the fraction of individuals who progress to infectious TB via the fast route is also determined by the proportion of individuals unvaccinated with the BCG vaccine. Hence, public health policy should take into cognisance the level of treatment facilities for the treatment of infectious TB cases in the population and the effectiveness of the BCG vaccination programme. With increasing (and sustained) treatment rates for TB infections, having a large proportion of infectious TB cases expeditiously getting treatment and increasing (and sustained) vaccination with the BCG vaccine with very high efficacy and very low waning ability induces a cut-back in the disease load in the population.

3.1.2 Analysis of $\mathcal{R}_{HS}$ [1]

Calculating the partial derivatives of $\mathcal{R}_{HS}$ as regards the parameters under analysis ($\zeta_S, N_e, \gamma, \phi, J_0$ and L_0) reveals, further, the impact of these parameters on schistosomiasis regulation in the populace. This gives

$$\frac{\partial \mathcal{R}_{HS}}{\partial \zeta_S} = -\frac{\alpha_1 \beta_J \beta_L \Lambda_H \Lambda_S \phi N_e \gamma}{2J_0 L_0 \mu_H \mu_J \mu_L \mu_S^2 (\alpha + \mu_H)(\zeta_S + \delta_S + \mu_H)^2 \mathcal{R}_{HS}} < 0. \tag{3.5}$$

Certainly, it is obvious from (3.5) that the partial derivative is unconditionally less than zero. Hence, effective treatment rate of schistosomiasis at the stage of infection will exert a positive effect in decreasing

the load of schistosomiasis in the populace, regardless of the values of the other parameters in the expression on the right-hand side of (3.5).

$$\frac{\partial \mathcal{R}_{HS}}{\partial N_e} = \frac{\alpha_1 \beta_J \beta_L \Lambda_H \Lambda_S \phi \gamma}{2J_0 L_0 \mu_J \mu_L \mu_S^2 (\alpha_1 + \mu_H)(\zeta_S + \delta_S + \mu_H)\mathcal{R}_{HS}} > 0. \tag{3.6}$$

However, we observe, from (3.6), that the number of schistososome eggs secreted by infectious human sub-population will exert a negative effect in decreasing the load of schistosomiasis in the populace, regardless of the values of the other parameters in the expression on the right-hand side of (3.6).

$$\frac{\partial \mathcal{R}_{HS}}{\partial \gamma} = \frac{\alpha_1 \beta_J \beta_L \Lambda_H \Lambda_S \phi N_e}{2J_0 L_0 \mu_J \mu_L \mu_S^2 (\alpha_1 + \mu_H)(\zeta_S + \delta_S + \mu_H)\mathcal{R}_{HS}} > 0. \tag{3.7}$$

We also observe, from (3.7), that the rate at which schistososome eggs (secreted by infectious human sub-population) favourably develop into miracidia will exert a negative effect in decreasing the load of schistosomiasis in the populace, regardless of the values of the other parameters in the expression on the right-hand side of (3.7).

$$\frac{\partial \mathcal{R}_{HS}}{\partial \phi} = \frac{\alpha_1 \beta_J \beta_L \Lambda_H \Lambda_S N_e \gamma}{2J_0 L_0 \mu_J \mu_L \mu_S^2 (\alpha_1 + \mu_H)(\zeta_S + \delta_S + \mu_H)\mathcal{R}_{HS}} > 0. \tag{3.8}$$

We further observe, from (3.8), that the cercarial production rate (by the infectious snail sub-population) will exert a negative effect in decreasing the load of schistosomiasis in the populace, regardless of the values of the other parameters in the expression on the right-hand side of (3.8).

$$\frac{\partial \mathcal{R}_{HS}}{\partial J_0} = -\frac{\alpha_1 \beta_J \beta_L \Lambda_H \Lambda_S \phi N_e}{2J_0 L_0 \mu_J \mu_L \mu_S^2 (\alpha_1 + \mu_H)(\zeta_S + \delta_S + \mu_H)\mathcal{R}_{HS}} < 0. \tag{3.9}$$

We also observe, from (3.9), that the saturation constant for the cercariae will exert a positive effect in decreasing the load of schistosomiasis in the populace, regardless of the values of the other parameters in the expression on the right-hand side of (3.9).

$$\frac{\partial \mathcal{R}_{HS}}{\partial L_0} = -\frac{\alpha_1 \beta_J \beta_L \Lambda_H \Lambda_S \phi N_e}{2J_0 L_0 \mu_J \mu_L \mu_S^2 (\alpha_1 + \mu_H)^2(\zeta_S + \delta_S + \mu_H)\mathcal{R}_{HS}} < 0. \tag{3.10}$$

We also observe, from (3.10), that the saturation constant for the miracidia will exert a positive effect in decreasing the burden of schistosomiasis in the community, irrespective of the values of the other parameters in the expression on the right-hand side of (3.10).

Further analysis of $\mathcal{R}_{HS}$ yields

$$\lim_{\substack{\zeta_S\to\infty \\ N_e\to 0 \\ \gamma\to 0}} \mathcal{R}_{HS} = 0. \tag{3.11}$$

The limit in (3.11) demonstrates the impact of a schistosomiasis control programme that concentrates on prompt and effective treatment of individuals with active schistosomiasis, reduction of the volume of schistosome eggs excreted by infectious individuals and reduction of the rate at which eggs secreted by infectious humans successfully become miracidia.

$$\lim_{\substack{\zeta_S\to\infty \\ J_0\to\infty \\ L_0\to\infty}} \mathcal{R}_{HS} = 0. \tag{3.12}$$

The limit in (3.12) demonstrates the impact of a schistosomiasis control programme that concentrates on prompt and effective treatment of individuals with active schistosomiasis and the elimination of both cercariae and miracidia from the aquatic reservoir that hosts them in the environment.

From the analysis of $\mathcal{R}_{HS}$ as seen in (3.5) - (3.10) and (3.11) - (3.12), respectively, we obtain the following result:

Lemma 3.3. *[1] The effective treatment rate (ζ_S) for the infectious stage of infection of the human sub-population, reduction of both the number of schistosome eggs secreted and the rate at which the excreted eggs favourably develop into miracidia, and the elimination of both cercariae and miracidia from the aquatic reservoir that hosts them in the environment will exert a positive effect in decreasing the schistosomiasis load among the populace populace, regardless of the values of the other parameters in the effective reproduction number.*

Further analysis of the threshold quantity, $\mathcal{R}_{HS}$, is carried out by investigating its sensitivity to certain key parameters, namely: the schistosomiasis treatment rate (ζ_S), the cercarial penetration rate (β_J), the number schistosome eggs secreted (N_e), the rate at which the eggs become miracidia (γ) well as the cercarial production rate (ϕ). Hence, we examine the contour plots (Figures 3 - 6) of $\mathcal{R}_{HS}$ as functions of ζ_S, β_J, N_e, γ and ϕ.

Figure 3 suggests that a low rate of cercarial penetration ($\phi = 28\%$) and an average rate at which the schistosome eggs become miracidia ($\gamma = 50\%$) (in the presence of treatment, with $\phi = 500$ and $\gamma = 0.8468$) is needed to abolish schistosomiasis in the populace. All regulatory policies hinged on the measures presented in Figure 3 will compel $\mathcal{R}_{HS} < 1$.

Figure 4 shows that an average level of the number of schistosome eggs secreted by humans ($N_e = 40\%$) coupled with an average cercarial production rate ($\phi = 40\%$), in the presence of treatment (with $N_e = 300$

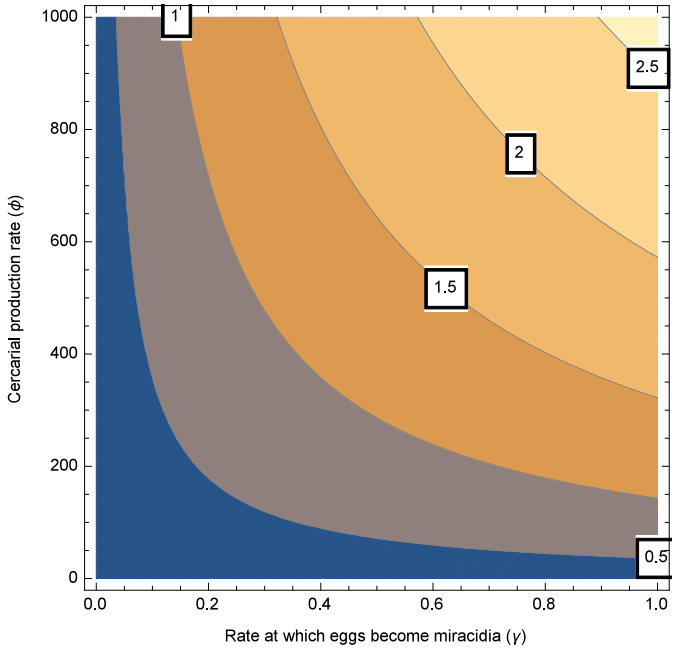

Figure 3: Contour plot of $\mathcal{R}_{HS}$ as a function of ϕ and γ [1].

and $\phi = 500$), is required to annihilate schistosomiasis in the populace. All regulatory policies hinged on the measures presented in Figure 4 will compel $\mathcal{R}_{HS} < 1$.

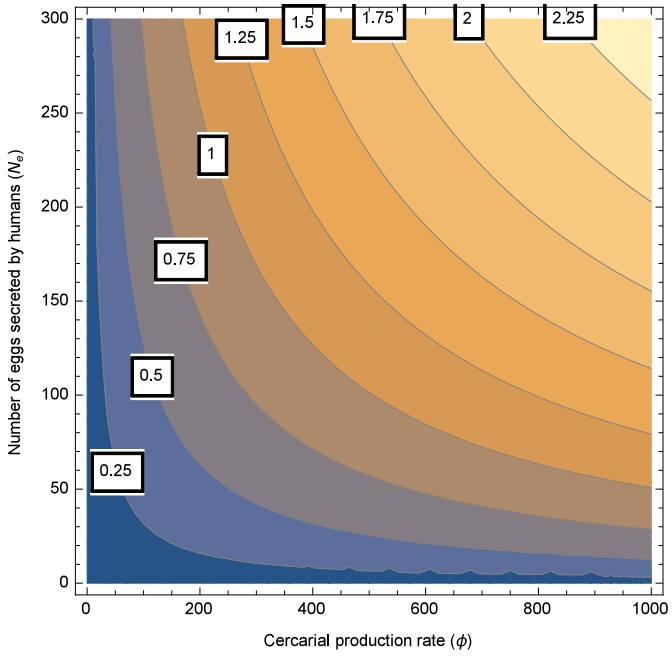

Figure 4: Contour plot of $\mathcal{R}_{HS}$ as a function of N_e and ϕ [3].

Figure 5 suggests that a moderate treatment level of humans with active schistosomiasis (60%) coupled with a low schistosomiasis transmission rate ($\beta_J = 1.70$) is needed to annihilate schistosomiasis from the populace. All regulatory policies hinged on the measures presented Figure 5 will compel $\mathcal{R}_{HS} < 1$.

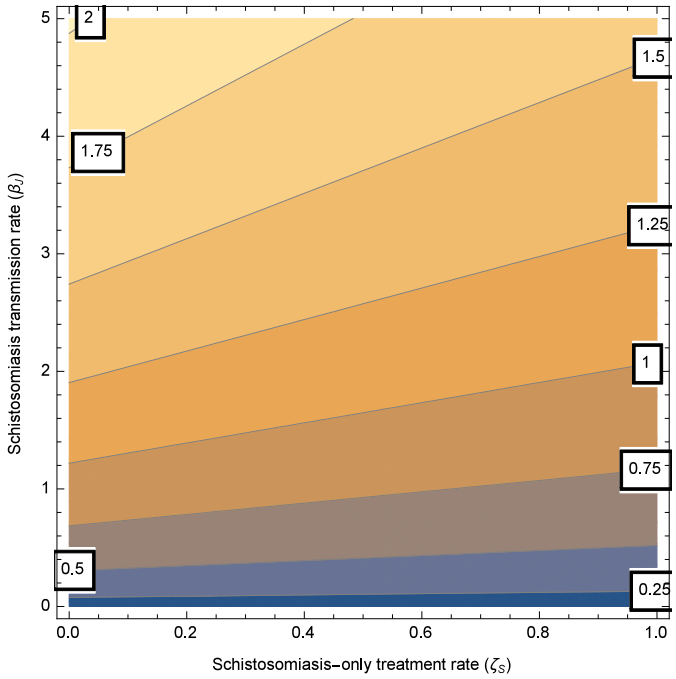

Figure 5: Contour plot of $\mathcal{R}_{HS}$ as a function of β_J and ζ_S [1].

Figure 6 suggests that a high treatment level ($\zeta_S = 60 - 80\%$) of actively-infected schistosomiasis cases and a low level of cercarial production rate ($\phi = 19 - 22\%$) are needed to annihilate schistosomiasis from the populace. All regulatory policies hinged on the measures presented in Figure 6 will compel $\mathcal{R}_{HS} < 1$.

In summary, the results from these contour plots suggest that the impact of the cercarial production, cercarial penetration, the number of schistosome eggs secreted and the successful conversion of the eggs to miracidia, on the burden of tuberculosis among the populace, is widely determined by the treatment levels for humans with active schistosomiasis. Hence, public health policy should take into account the level of treatment facilities available. With increasing (and sustained) treatment rates for schistosomiasis infections, having a large proportion of infectious schistosomiasis patients expeditiously getting treatment will result in a contraction of the disease load among the populace [1].

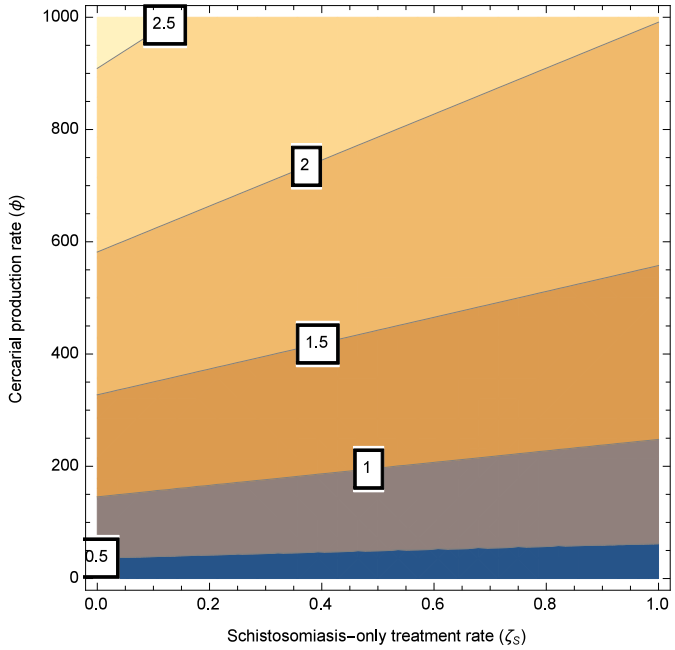

Figure 6: Contour plot of $\mathcal{R}_{HS}$ as a function of ϕ and ζ_S [3].

4 Simulations

We investigate, herein, the uncertainty and sensitivity of the parameters of the model system (2.3) [3] dependent on the effective reproduction number as output function. We also present numerical simulation results which demonstrates the effect of changing certain key parameters on the total disease incidence in a population. The work done in this section is based on values of the parameters given in Tables 7 and 8.

4.1 Uncertainty and Sensitivity Analysis

The model system (2.3) has 61 parameters, and it is expected that uncertainties will arise in estimating parameter values deployed to simulate the model system. To evaluate the extent of these uncertainties and to locate those parameters that exert the strongest influence on the population dynamics of tuberculosis-schistosomiasis co-infection in the presence of vaccination with an imperfect BCG vaccine as a measure of prevention of TB infection.

To achieve this purpose, we carry out local sensitivity evaluation by calculating the sensitivity index, which is a partial derivative of the output function dependent on the input parameters [20]. Taking the effective reproduction number, $\mathcal{R}_{TS}^{\mathcal{V}}$ as the output function and g_i, an input parameter, the sensitivity

Table 4: Parameter values (along with ranges) of the system (2.3) [3]

Parameters	Values	Sample ranges	References
μ_H	0.02041 year^{-1}	[0.0143, 0.03]	[41]
Λ_H	3 868 900 year^{-1}	[3,000,000, 4,000,000]	[14]
β_T	Variable year^{-1}	[0, 2]	Assumed
ζ_{TS}	2.5 year^{-1}	[1, 3]	Assumed
ξ	0.075 year^{-1}	[0, 1]	[16]
p	0.1 year^{-1}	[0.05, 0.3]	[38]
f	0.1 year^{-1}	[0, 0.005]	[38]
m	0.1 year^{-1}	[0, 3]	[38]
π_1	0.4 year^{-1}	[0, 1]	[16]
π_2	0.45 year^{-1}	[0, 1]	[16]
π_3	0.5 year^{-1}	[0, 1]	[16]
k_1	0.005 year^{-1}	[0.005, 0.05]	[7]
k_2	0.005 year^{-1}	[0.005, 0.05]	[7]
k_3	0.005 year^{-1}	[0.005, 0.05]	[7]
ζ_T	0.75 year^{-1}	[0, 1]	Assumed
ζ_{T1}	0.75 year^{-1}	[0.5, 1]	[30]
ζ_{T2}	0.75 year^{-1}	[0.5, 1]	[30]
ζ_{T3}	0.75 year^{-1}	[0.5, 1]	[30]
ζ_R	0.75 year^{-1}	[0.5, 1]	[30]
ζ_{R1}	0.75 year^{-1}	[0.5, 1]	[30]
ζ_S	0.23 year^{-1}	[0.2, 0.5]	[19]
ζ_{S1}	0.23 year^{-1}	[0.2, 0.5]	[19]
ζ_{S2}	0.23 year^{-1}	[0.2, 0.5]	[19]
ζ_{S3}	0.23 year^{-1}	[0.2, 0.5]	[19]

index can be computed as $\partial \mathcal{R}^{\mathcal{V}}_{\mathcal{TS}}/\partial g_i$. The normalized sensitivity index, $\Omega^{\mathcal{R}^{\mathcal{V}}_{\mathcal{TS}}}_{g_i}$, of $\mathcal{R}^{\mathcal{V}}_{\mathcal{TS}}$, with respect to parameter g_i at a fixed rate, g^0 [**?**] is

$$\Omega^{\mathcal{R}^{\mathcal{V}}_{\mathcal{TS}}}_{g_i} = \frac{\partial \mathcal{R}^{\mathcal{V}}_{\mathcal{TS}}}{\partial g_i} \times \frac{g_i}{\mathcal{R}^{\mathcal{V}}_{\mathcal{TS}}}\Big|_{g_i=g^0}. \tag{4.1}$$

Employing the parameter values in Tables 4 and 5, we proceed to compute the sensitivity indices employing (4.1). We observe that there are twenty-two (25) parameters in the effective reproduction

Table 5: Parameter values (along with ranges) of the system (2.3) [3] (cont'd)

Parameters	Values	Sample ranges	References
ω	0.2 year^{-1}	[0, 1]	Assumed
θ_V	0.08 year^{-1}	[0.067, 0.1]	[4, 26]
ϵ_1	0.9 year^{-1}	[0, 1]	Assumed
δ_T	0.1 year^{-1}	[0, 0.5]	[6]
δ_R	0.1 year^{-1}	[0, 0.5]	[6]
δ_S	1.4 year^{-1}	[0.365, 2.19]	[25]
α_1	6.5 year^{-1}	[0, 10]	[25]
α_2	6.5 year^{-1}	[0, 10]	[25]
α_3	6.5 year^{-1}	[0, 10]	[25]
ψ	0.85 year^{-1}	[0.05, 0.85]	Assumed
σ	0.5 year^{-1}	[0, 1]	Assumed
χ_1	0.65 year^{-1}	[0, 1]	Assumed
χ_2	0.85 year^{-1}	[0, 1]	Assumed
η_1	2.0 year^{-1}	[0, 3]	Assumed
η_2	4.0 year^{-1}	([0, 5]	Assumed
Θ_{RT}	0.5 year^{-1}	[0, 1]	Assumed
Θ_{RS1}	1.5 year^{-1}	[0, 3]	Assumed
Θ_{RS2}	1.5 year^{-1}	[0, 3]	Assumed
Π_1	1.8 year^{-1}	[0, 3]	Assumed
Π_2	2.0 year^{-1}	[0, 3]	Assumed
υ_1	0.001 year^{-1}	[0, 1]	Assumed
υ_2	0.002 year^{-1}	[0, 1]	Assumed
υ_3	0.003 year^{-1}	[0, 1]	Assumed
μ_S	0.5 year^{-1}	[0, 1]	[19]
Λ_S	73,000 year^{-1}	[73,000, 109,500]	[12]
ϵ	182.5 year^{-1}	[0, 182.5]	[12]
β_L	1.475 year^{-1}	[0, 2]	Assumed
L_0	10^8 year^{-1}	[9×10^7, 1×10^8]	[12]
N_e	300 year^{-1}	[0, 800]	[12]
γ	0.8468 year^{-1}	[0, 1]	[12]
μ_L	328.5 year^{-1}	[100, 400]	[12]
β_J	4.19 year^{-1}	[0, 5]	Assumed
J_0	9×10^7 year^{-1}	[8×10^7, 9×10^7]	[12]
μ_J	3.0 year^{-1}	[0, 3]	[12]
τ_1	0.1 year^{-1}	[0, 1]	Assumed
τ_2	0.2 year^{-1}	[0, 1]	Assumed
ϕ	500 year^{-1}	[0, 1,000]	[12]

number, $\mathcal{R}^{\mathcal{V}}_{\mathcal{TS}} = max\{\mathcal{R}^{\mathcal{V}}_{\mathcal{HT}}, \mathcal{R}_{\mathcal{HS}}\}$, of the TB-schistosomiasis co-infection model (2.3). We shall investigate the sensitivity of these 25 parameters to $\mathcal{R}^{\mathcal{V}}_{\mathcal{HT}}$ and $\mathcal{R}_{\mathcal{HS}}$, respectively.

When we set $\mathcal{R}^{\mathcal{V}}_{\mathcal{HT}}$ to be our output function in (4.1), the two parameters with the highest sensitivity indices were: the rate of TB transmission (β_T) and the rate of TB treatment (ζ_T). See Table 6 and Figure 7 for details.

Table 6: Sensitivity indices for the parameters of the model (2.3) using the effective reproductive number ($\mathcal{R}^{\mathcal{V}}_{\mathcal{HT}}$) as response function.

Parameters	$\mathcal{R}^{\mathcal{V}}_{\mathcal{HT}}$
β_T	**+1.0000**
θ_V	+0.1373
κ_1	+0.2514
ω	+0.0431
p	+0.0385
ϵ_1	–0.1648
μ_H	–0.4121
ζ_T	**–0.8617**
δ_T	–0.1149

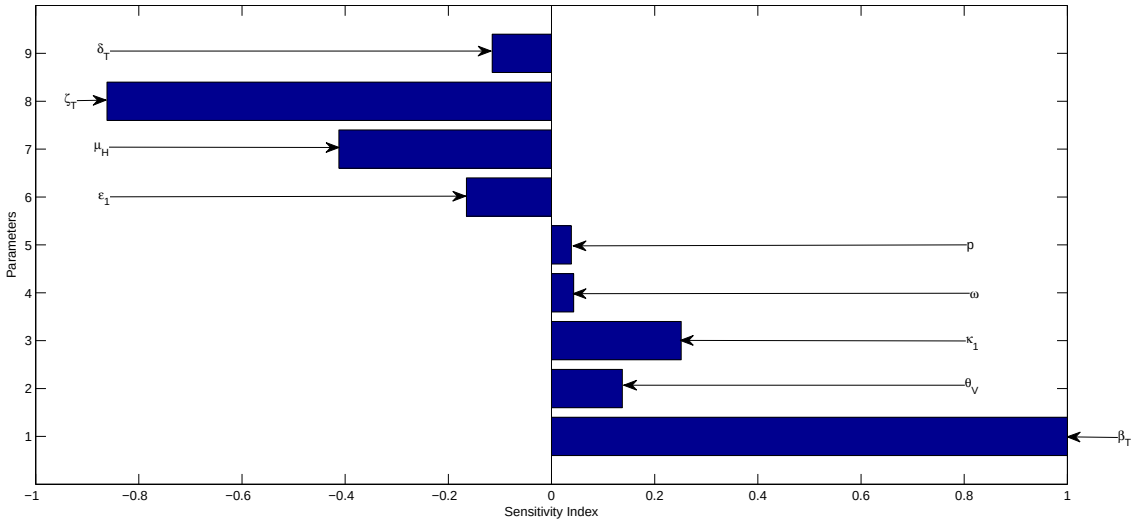

Figure 7: Local sensitivity analysis of $\mathcal{R}^{V}_{HT}$.

When we adopt $\mathcal{R}_{\mathcal{HS}}$ as our output function in (4.1), the thirteen parameters with the highest

sensitivity indices were: the snail mortality rate (μ_S), the rate of cercarial infection (β_J), the miracidial infection rate (β_L), the human recruitment rate (Λ_H), the snail recruitment rate (Λ_S), the number of eggs secreted by humans with active schistosomiasis (N_e), the rate at which secreted eggs successfully become miracidia (γ), the rate of cercarial production (ϕ), the saturation constant for cercariae (J_0), the saturation constant for the miracidia (L_0), the natural death rate of humans (μ_H), the cercarial death rate (μ_J), and the miracidial death rate (μ_L). See Table 7 and Figure 8 for details.

Table 7: Sensitivity indices for the parameters of the model (2.3) using the effective reproductive number ($\mathcal{R}_{\mathcal{HS}}$) as response function [3].

Parameters	$\mathcal{R}_{\mathcal{HS}}$	Parameters	$\mathcal{R}_{\mathcal{HS}}$
α_1	+0.0016	J_0	**–0.5000**
β_J	**+0.5000**	L_0	**–0.5000**
β_L	**+0.5000**	μ_H	**–0.5000**
Λ_H	**+0.5000**	μ_J	**–0.5000**
Λ_S	**+0.5000**	μ_L	**–0.5000**
N_e	**+0.5000**	μ_S	**–1.0000**
γ	**+0.5000**	ζ_S	–0.0697
ϕ	**+0.5000**	δ_S	–0.4241

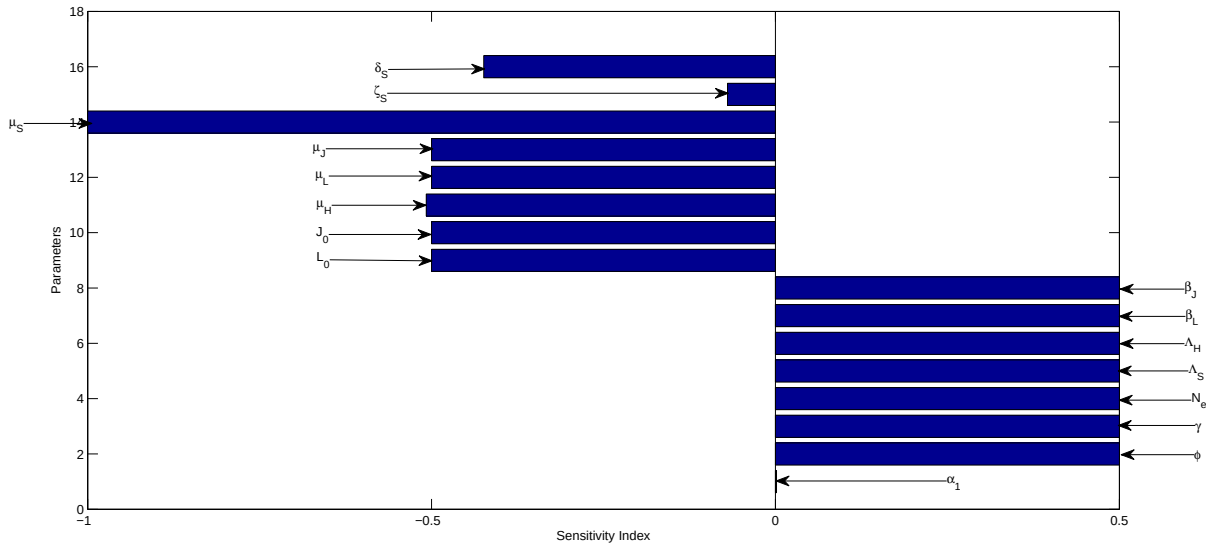

Figure 8: Local sensitivity analysis of $\mathcal{R}_{HS}$.

5 Conclusion

Local sensitivity analysis was carried out on key parameters using the effective reproduction number as a response function in [3]. Fifteen (15) parameters that had the highest indices were: the TB transmission rate (β_T), the snail mortality rate (μ_S), the TB treatment rate (ζ_T), the cercarial infection rate (β_J), the miracidial infection rate (β_L), the human recruitment rate (Λ_H), the nail recruitment rate (Λ_S), the number of eggs secreted by humans with active schistosomiasis (N_e), the rate at which secreted eggs successfully become miracidia (γ), the cercarial production rate (ϕ), the saturation constant for cercariae (J_0), the saturation constant for the miracidia (L_0), the natural death rate of humans (μ_H), the cercarial death rate (μ_J), and the miracidial death rate (μ_L).

This study has shown that TB and schistosomiasis control programmes that support the respective treatment of active cases of both diseases, vaccination of susceptible humans with the BCG vaccine (with high vaccine efficacy and low vaccine waning) against TB infection and the deliberate reduction of unvaccinated human individuals who are susceptible to TB should be tenaciously pursued, since it has been shown that such programmes could result in significant decrease in the burden of TB-schistosomiasis co-infection in the population.

References

[1] Ako, I. I. (2024). Uncertainty and sensitivity analysis of the effective reproduction number for a deterministic mathematical model for tuberculosis-schistosomiasis co-infection dynamics. *Transactions of the Nigerian Association of Mathematical Physics*, *20*, 45–60. http://doi.org/10.60787/tnamp.v20.378

[2] Ako, I. I., & Olowu, O. O. (2024). Causes of backward bifurcation in a tuberculosis-schistosomiasis co-infection dynamics. *Earthline Journal of Mathematical Sciences*, *14*(4), 655–695. https://doi.org/10.34198/ejms.14424.655695

[3] Ako, I. I., & Omoregie, R. U. (2025). Mathematical analysis of a tuberculosis-schistosomiasis co-infection model with vaccination and treatment. *Earthline Journal of Mathematical Sciences*, *15*(4), 649–683. https://doi.org/10.34198/ejms.15425.649683

[4] Anderson, E. J., Webb, E. L., Mawa, P. A., Kizza, M., Lyadda, N., Nampijja, M., & Elliot, A. M. (2012). The influence of BCG vaccine strain on mycobacteria-specific and non-specific immune responses in a prospective cohort of infants in Uganda. *Vaccine*, *30*, 2083–2089. https://doi.org/10.1016/j.vaccine.2012.01.053

[5] Barbour, A. D. (1982). Schistosomiasis. In R. M. Anderson (Ed.), *Population dynamics of infectious diseases* (pp. 180–208). Chapman and Hall. https://doi.org/10.1007/978-1-4899-2901-3_6

[6] Bhunu, C. P., Garira, W., & Magombedze, G. (2009). Mathematical analysis of a two-strain HIV/AIDS model with antiretroviral treatment. *Acta Biotheoretica*, *57*(3), 361–381. https://doi.org/10.1007/s10441-009-9080-2

[7] Blower, S. M., McLean, A. R., Porco, T. C., Small, P. M., Hopewell, P. C., Sanchez, M. A., & Moss, A. R. (1995). The intrinsic transmission dynamics of tuberculosis epidemics. *Nature Medicine*, *1*, 815–821. https://doi.org/10.1038/nm0895-815

[8] Cariboni, J., Gatelli, D., Liska, R., & Saltelli, A. (2007). The role of sensitivity analysis in ecological modelling. *Ecological Modelling*, *203*(1-2), 167. https://doi.org/10.1016/j.ecolmodel.2005.10.045

[9] Castillo-Chavez, C., & Song, B. (2004). Dynamical models of tuberculosis and their applications. *Mathematical Biosciences and Engineering*, *1*(2), 361–404. https://doi.org/10.3934/mbe.2004.1.361

[10] Chen, Z., Zou, L., Shen, D., Zhang, W., & Ruan, S. (2010). Mathematical modelling and control of schistosomiasis in Hubei Province, China. *Acta Tropica*, *115*, 119–125. https://doi.org/10.1016/j.actatropica.2010.02.012

[11] Chitnis, N., Hyman, J. M., & Cushing, J. M. (2008). Determining important parameters in the spread of malaria through the sensitivity analysis of a mathematical model. *Bulletin of Mathematical Biology*, *70*(5), 1272–1296. https://doi.org/10.1007/s11538-008-9299-0

[12] Chiyaka, E., & Garira, W. (2009). Mathematical analysis of the transmission dynamics of schistosomiasis in the human-snail hosts. *Journal of Biological Systems*, *17*, 397–423. https://doi.org/10.1142/S0218339009002910

[13] Cohen, J. E. (1977). Mathematical models of schistosomiasis. *Annual Review of Ecology and Systematics*, *8*, 209–233. https://doi.org/10.1146/annurev.es.08.110177.001233

[14] Countrymeters. (2017). Nigeria population. https://countrymeters.info/en/Nigeria

[15] Diaby, M. A., & Iggidr, A. (2016). A mathematical analysis of a model with mating structure. *Proceedings of CARI*, *246*, 402–411.

[16] Feng, Z., Castillo-Chavez, C., & Capurro, A. F. (2000). A model for tuberculosis with exogenous reinfection. *Theoretical Population Biology*, *57*, 235–247. https://doi.org/10.1006/tpbi.2000.1451

[17] Feng, Z., Curtis, J., & Minchella, D. J. (2001). The influence of drug treatment on the maintenance of schistosome genetic diversity. *Journal of Mathematical Biology*, *43*, 52–68. https://doi.org/10.1007/s002850100092

[18] Feng, Z., Li, C.-C., & Milner, F. A. (2002). Schistosomiasis models with density dependence and age of infection in snail dynamics. *Mathematical Biosciences*, *177-178*, 271–286. https://doi.org/10.1016/S0025-5564(01)00115-8

[19] Feng, Z., Eppert, A., Milner, F. A., & Minchella, D. J. (2004). Estimation of parameters governing the transmission dynamics of schistosomes. *Applied Mathematics Letters*, *17*, 1105–1112. https://doi.org/10.1016/j.aml.2004.02.002

[20] Lutambi, A. M., Penny, M. A., Smith, T., & Chitnis, N. (2013). Mathematical modelling of mosquito dispersal in a heterogeneous environment. *Mathematical Biosciences*, *241*, 198–216. https://doi.org/10.1016/j.mbs.2012.11.013

[21] Macdonald, G. (1965). The dynamics of helminth infections with special reference to schistosomes. *Transactions of the Royal Society of Tropical Medicine and Hygiene*, *59*(5), 489–506. https://doi.org/10.1016/0035-9203(65)90152-5

[22] Milner, F. A., & Zhao, R. (2008). A deterministic model of schistosomiasis with spatial structure. *Mathematical Biosciences and Engineering*, *5*(3), 505–522. http://www.mbejournal.org/

[23] Monin, L., Griffiths, K. L., Lam, W. Y., Gopal, R., Kang, D. D., Ahmed, M., Rajamanickam, A., Cruz-Lagunas, A., Zúñiga, J., Babu, S., Kolls, J. K., Mitreva, M., Rosa, B. A., Ramos-Payan, R., Morrison, T. E., Murray, P. J., Rangel-Moreno, J., Pearce, E. J., & Khader, S. A. (2015). Helminth-induced arginase-1 exacerbates lung inflammation and disease severity in tuberculosis. *The Journal of Clinical Investigation*, *125*(12), 4699–4713. https://doi.org/10.1172/JCI77378

[24] Mushayabasa, S., & Bhunu, C. P. (2011). Modelling schistosomiasis and HIV/AIDS codynamics. *Computational and Mathematical Methods in Medicine*, *2011*, Article ID 846174. https://doi.org/10.1155/2011/846174

[25] Ngarakana-Gwasira, E. T., Bhunu, C. P., Masocha, M., & Mashonjowa, E. (2016). Transmission dynamics of schistosomiasis in Zimbabwe: A mathematical and GIS approach. *Communications in Nonlinear Science and Numerical Simulation*, *35*, 137–147. https://doi.org/10.1016/j.cnsns.2015.11.005

[26] Nguipdop-Djomo, P., Heldal, E., Rodrigues, L. C., Abubakar, I., & Mangtani, P. (2015). Duration of BCG protection against tuberculosis and change in effectiveness with time since vaccination in Norway: A retrospective population-based cohort study. *The Lancet Infectious Diseases*, *16*(2), 219–226. https://doi.org/10.1016/S1473-3099(15)00400-4

[27] Okosun, K. O., & Smith, R. (2017). Optimal control analysis of malaria-schistosomiasis co-infection dynamics. *Mathematical Biosciences and Engineering*, *14*(2), 377–405. https://doi.org/10.3934/mbe.2017024

[28] Okuonghae, D. (2013). A mathematical model of tuberculosis transmission with heterogeneity in disease susceptibility and progression under a treatment regime for infectious cases. *Applied Mathematical Modelling*, *37*, 6786–6808. https://doi.org/10.1016/j.apm.2013.01.039

[29] Okuonghae, D. (2014). Lyapunov functions and global properties of some tuberculosis models. *Journal of Applied Mathematics and Computing*. https://doi.org/10.1007/s12190-014-0811-4

[30] Okuonghae, D., & Aihie, V. (2008). Case detection and direct observation therapy strategy (DOTS) in Nigeria: Its effect on TB dynamics. *Journal of Biological Systems*, *16*(1), 1–31. https://doi.org/10.1142/S0218339008002344

[31] Okuonghae, D., & Aihie, V. U. (2010). Optimal control measures for tuberculosis mathematical models including immigration and isolation of infective. *Journal of Biological Systems*, *18*(1), 17–54. https://doi.org/10.1142/S0218339010003160

[32] Okuonghae, D., & Ikhimwin, B. O. (2016). Dynamics of a mathematical model for tuberculosis with variability in susceptibility and disease progressions due to difference in awareness level. *Frontiers in Microbiology*, *6*, 1530. https://doi.org/10.3389/fmicb.2015.01530

[33] Okuonghae, D., & Korobeinikov, A. (2007). Dynamics of tuberculosis: The effect of Direct Observation Therapy Strategy (DOTS) in Nigeria. *Mathematical Modelling of Natural Phenomena*, *2*(1), 101–113. https://doi.org/10.1051/mmnp:2008013

[34] Okuonghae, D., & Omosigho, S. E. (2011). Analysis of a mathematical model for tuberculosis: What could be done to increase case detection. *Journal of Theoretical Biology*, *269*, 31–45. https://doi.org/10.1016/j.jtbi.2010.09.044

[35] Olowu, O., & Ako, I. (2023). Computational investigation of the impact of availability and efficacy of control on the transmission dynamics of schistosomiasis. *International Journal of Mathematical Trends and Technology*, *69*(8), 1–9. https://doi.org/10.14445/22315373/IJMTT-V69I8P501

[36] Olowu, O., Ako, I. I., & Akhaze, R. I. (2021). Theoretical study of a two patch metapopulation schistosomiasis model. *Transactions of the Nigerian Association of Mathematical Physics*, *14* (January-March Issue), 53–68.

[37] Olowu, O., Ako, I. I., & Akhaze, R. I. (2021). On the analysis of a two patch schistosomiasis model. *Transactions of the Nigerian Association of Mathematical Physics*, *14* (January-March Issue), 69–78.

[38] Porco, T. C., & Blower, S. M. (1998). Quantifying the intrinsic transmission dynamics of tuberculosis. *Theoretical Population Biology*, *54*, 117–132. https://doi.org/10.1006/tpbi.1998.1366

[39] Qi, L., & Cui, J. (2013). A schistosomiasis model with mating structure. *Abstract and Applied Analysis*, *2013*, Article ID 741386. https://doi.org/10.1155/2013/741386

[40] Qi, L., Xue, M., Cui, J., Wang, Q., & Wang, T. (2018). Schistosomiasis model and its control in Anhui Province. *Bulletin of Mathematical Biology*, *80*, 2435–2451. https://doi.org/10.1007/s11538-018-0474-7

[41] UNAIDS-WHO. (2004). *Epidemiological fact sheet*. http://www.unaids.org

[42] van den Driessche, P., & Watmough, J. (2002). Reproduction numbers and sub-threshold endemic equilibria for compartmental models of disease transmission. *Mathematical Biosciences*, *180*, 29–48. https://doi.org/10.1016/S0025-5564(02)00108-6

[43] Waaler, H., Geser, A., & Andersen, S. (1962). The use of mathematical models in the study of the epidemiology of tuberculosis. *American Journal of Public Health and the Nations Health*, *52*(6), 1002–1013. https://doi.org/10.2105/AJPH.52.6.1002

[44] World Health Organization (WHO). (2023). *Global tuberculosis report 2023*. World Health Organization Press.

[45] World Health Organization (WHO). (2023). *Schistosomiasis factsheet 2023*. World Health Organization Press.

[46] World Health Organization (WHO). (2025). *Tuberculosis factsheet 2025*. World Health Organization Press.

[47] Woolhouse, M. E. J. (1991). On the application of mathematical models of schistosome transmission dynamics I: Natural transmission. *Acta Tropica*, *49*, 241–262. https://doi.org/10.1016/0001-706X(91)90077-W

[48] Zhao, R., & Milner, F. A. (2008). A mathematical model of *Schistosoma mansoni* in *Biomphalaria glabrata* with control strategies. *Bulletin of Mathematical Biology*, *70*(7), 1886–1905. https://doi.org/10.1007/s11538-008-9330-5

[49] Zou, L., & Ruan, S. (2015). Schistosomiasis transmission and control in China. *Acta Tropica*, *143*, 51–57. https://doi.org/10.1016/j.actatropica.2014.12.004